

Fusing Structural and Functional Connectivities using Disentangled VAE for Detecting MCI

Qiankun Zuo^{1,8}, Yanfei Zhu²(✉), Libin Lu³, Zhi Yang⁴, Yuhui Li⁵, and Ning Zhang^{6,7}

¹ School of Information Engineering, Hubei University of Economics, Wuhan 430205, China

² School of Foreign Languages, Sun Yat-sen University, Guangzhou 510275, China

³ School of Mathematics and Computer Science, Wuhan Polytechnic University, Wuhan 430023, China

⁴ College of Electronics and Information Engineering, Sichuan University, Chengdu 610065, China

⁵ Goertek Inc., Beijing 100083, China

⁶ Beijing SmartDoor Technology Co., Ltd., Beijing 101399, China

⁷ Beijing Zhongke Ruijian Technology Co., Ltd., Beijing 100088, China

⁸ Zhuhai Shi Jiexinsoftware Technology Co., Ltd., Zhuhai 519090, China

Corresponding email: zhuyf53@mail.sysu.edu.cn

Abstract. Brain network analysis is a useful approach to studying human brain disorders because it can distinguish patients from healthy people by detecting abnormal connections. Due to the complementary information from multiple modal neuroimages, multimodal fusion technology has a lot of potential for improving prediction performance. However, effective fusion of multimodal medical images to achieve complementarity is still a challenging problem. In this paper, a novel hierarchical structural-functional connectivity fusing (HSCF) model is proposed to construct brain structural-functional connectivity matrices and predict abnormal brain connections based on functional magnetic resonance imaging (fMRI) and diffusion tensor imaging (DTI). Specifically, the prior knowledge is incorporated into the separators for disentangling each modality of information by the graph convolutional networks (GCN). And a disentangled cosine distance loss is devised to ensure the disentanglement's effectiveness. Moreover, the hierarchical representation fusion module is designed to effectively maximize the combination of relevant and effective features between modalities, which makes the generated structural-functional connectivity more robust and discriminative in the cognitive disease analysis. Results from a wide range of tests performed on the public Alzheimer's Disease Neuroimaging Initiative (ADNI) database show that the proposed model performs better than competing approaches in terms of classification evaluation. In general, the proposed HSCF model is a promising model for generating brain structural-functional connectivities and identifying abnormal brain connections as cognitive disease progresses.

Keywords: Structural-Functional fusion · Hierarchical representation · Disentangled learning · Graph convolutional network · MCI.

1 Introduction

Alzheimer’s disease (AD) is one of the most prevalent progressive and irreversible degenerative disorders affecting the elderly, where the initial onset is considered to be mild cognitive impairment (MCI). Memory loss, aphasia, and other declining brain functions represent MCI-related symptoms and are indicative of pathological changes [1]. According to literature [2], the AD conversion rate from MCI is much higher than in normal people. In addition to making AD patients more depressed and anxious, it also lowers their quality of life and places a heavy financial burden on their families due to the high cost of care [3]. Furthermore, there is still no effective treatment for the illness [4]. Early diagnosis and treatment of patients with MCI can effectively slow their progression to AD. Therefore, developing an effective machine learning model for analyzing scanned medical imaging and other field applications for disease detection has attracted growing attention [5–15].

When the human brain completes a certain task, multiple brain regions need to interact with each other, so studying cognitive diseases from the perspective of brain connectivity is more explanatory. Brain networks are based on graph theory, where nodes usually represent neurons or regions of interest (ROIs), and edges represent the relationships between nodes (i.e., brain regions) [16]. Disease-related information can be conveyed in various ways by multiple modal images [17–20]. fMRI (functional magnetic resonance imaging) records brain activity and can reveal abnormal functional connectivity (FC) associated with disease [21, 22]. White matter fiber bundles in the brain can be recorded using diffusion tensor imaging (DTI), which can reveal abnormal structural connectivity (SC) between different brain regions [23, 24]. Compared with the traditional imaging-based method in MCI diagnosis [25–30], the connectivity-based methods show superior performance in accuracy evaluation by graph convolutional networks (GCN) [31, 32]. Researchers either use SC or FC to perform an early AD diagnosis clinically. For example, Zuo et al. [33] designed a transformer-based network to construct FC from functional MRI and improve MCI diagnosis accuracy compared with empirical methods. Since both fMRI and DTI can explore complementary information in patients, multimodal fusion has produced superior results in MCI diagnosis [34–36]. The work in [37] has proved the success of fusing SC and FC in MCI prediction. They utilized the local weighted clustering coefficients to adaptively fuse the functional and structural information, thus enhancing the disease diagnosis. This shows that fusing multimodal brain networks is promising and is becoming a hot topic in cognitive disease analysis [38–40]. However, the information from one modality may act as noise to prevent the expression of the other modality in previous approaches, which always combine the disentangled information of multimodal information. Consequently, minimizing the components that can have a detrimental impact on one another during the fusion process is the key to efficiently merging DTI and fMRI data.

The variational autoencoder (VAE) is one of the most generative methods [41–43] in information fusion by encoding features into latent representations, and the graph convolutional network (GCN) has a strong advantage in

constructing topological features. Inspired by the observations, in this paper, a novel hierarchical structural-functional connectivity fusion (HSCF) model is proposed to construct brain structural-functional connectivity matrices and predict abnormal brain connections based on functional magnetic resonance imaging (fMRI) and diffusion tensor imaging (DTI). The main advantages of this paper are the following: (1) The prior knowledge is incorporated into the separators for disentangling each modal information by GCN, which can separate the connectivity information in topological space and is more suitable for downstream fusion. (2) The hierarchical representation fusion module is designed to effectively maximize the combination of relevant and effective features between modalities, which makes the generated structural-functional connectivity more robust and discriminative in the cognitive disease analysis. Comprehensive results on the Alzheimer’s Disease Neuroimaging Initiative (ADNI) database show that the performance of the proposed model outperforms other competitive methods in terms of classification tasks.

2 Proposed Method

2.1 Disentangled VAE

The input to our framework is the graph data, where nodes represent the ROIs and edges represent the SC or FC. To simplify the description, we denote the SC and FC as the \mathbf{A}_1 and \mathbf{A}_2 respectively. Both SC and FC have the dimension size $N \times N$. The N represents the total number of brain regions studied in our study. The prior knowledge refers to the relative volume of anatomical brain regions, and we construct the node feature (NF) by translating each ROI’s volume into a one-hot vector. The NF is denoted as \mathbf{X} with a size of $N \times N$.

The framework is shown in Fig. 1. The disentangled VAE consists of four separators and four reconstructors. As an example, consider the distangled structural connectivity. The two separators are S_{ss} and S_{su} , where each of them takes \mathbf{A}_1 and \mathbf{X} as input and outputs the latent variables. The difference is that the former learns the structural-specific component (μ_{ss}, σ_{ss}) , while the latter learns the universal component (μ_{su}, σ_{su}) . The network structure of them contains three GCN layers: the first two layers have hidden dimensions of 64 and 32, respectively; the last layer has hidden dimensions of 16. Except for the last layer, the *ReLU* activation function is applied to all GCN layers. The computation procedure can be defined as follows:

$$\mu_{ss}, \sigma_{ss} = S_{ss}(\mathbf{A}_1, \mathbf{X}); \mu_{su}, \sigma_{su} = S_{su}(\mathbf{A}_1, \mathbf{X}) \quad (1)$$

$$\mu_{ff}, \sigma_{ff} = S_{ff}(\mathbf{A}_2, \mathbf{X}); \mu_{fu}, \sigma_{fu} = S_{su}(\mathbf{A}_2, \mathbf{X}) \quad (2)$$

here, each pair of latent variables has the same dimension $N \times 16$. The latent variable pairs can be considered a standard normal distribution, where we can obtain the latent representations by sampling operations. Supposing that the latent representations are \mathbf{Z}_{ss} , \mathbf{Z}_{su} , \mathbf{Z}_{ff} , and \mathbf{Z}_{fu} , we can recover the SC and

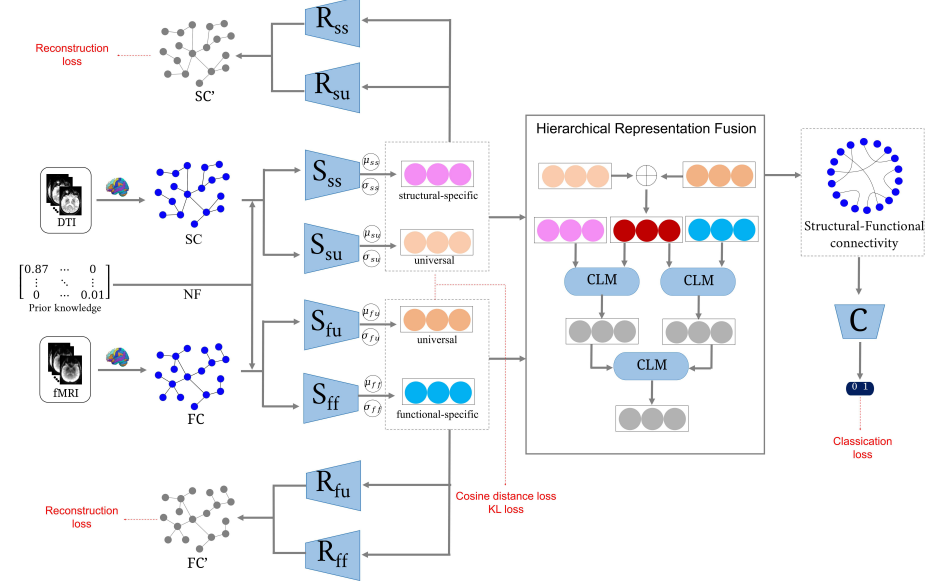


Fig. 1. The framework of the proposed HSCF using DTI and fMRI. It consists of three parts: the encoders, the decoders, and the hierarchical representation fusion.

FC by the reconstructors. The structure of the reconstructor has an N filter with a kernel size of 16×1 . The final output is the matrix inner product, followed by a *sigmoid* activation function. The fomulua can be expressed by:

$$\mathbf{A}'_1 = 0.5(\mathbf{A}_{s1} + \mathbf{A}_{s2}) \quad (3)$$

$$\mathbf{A}_{s1} = R_{ss}(\mathbf{Z}_{ss}), \mathbf{A}_{s2} = R_{su}(\mathbf{Z}_{su}) \quad (4)$$

$$\mathbf{A}'_2 = 0.5(\mathbf{A}_{f1} + \mathbf{A}_{f2}) \quad (5)$$

$$\mathbf{A}_{f1} = R_{ff}(\mathbf{Z}_{ff}), \mathbf{A}_{f2} = R_{fu}(\mathbf{Z}_{fu}) \quad (6)$$

2.2 Hierarchical Representation Fusion

The disentangled representations are combined to generate structural-functional connectivity for fusing complementary information. The hierarchical representation fusion (HRF) consists of three stages: (1) fusing the universal representations to obtain phase-1 representation; (2) partially fusing the phase-1 representation with modality-specific representations using connectivity linear mapping (CLM); this stage outputs phase-2 representations; and (3) continuing to incorporate the phase-2 representations to obtain phase-3 representation. The CLM consists of a two-layer multilayer perceptron (MLP). The output dimension of each layer is the same as the latent variable. The generated structural-functional connectivity is defined as:

$$\mathbf{A}_m = SFC = HRF(\mathbf{Z}_{ss}, \mathbf{Z}_{su}, \mathbf{Z}_{ff}, \mathbf{Z}_{fu}) \quad (7)$$

The classifier C shares the same structure with the work in [33]. The input of C is the generated SFC and NF.

2.3 Loss Functions

The Kullback-Leibler (KL) divergence and reconstruct loss must be monitored during the training process to keep the VAE-based model stable and robust. The generated structural-functional connectivity must be discriminative after disentangling and fusing the fMRI and DTI. We design four hybrid loss functions: the KL loss (L_{kl}), the reconstruct loss (L_{rec}), the distangled cosine distance loss (L_{cos}), and the classification loss (L_{cls}). They are defined as follows:

$$L_{kl} = KL(\mathbf{Z}_{ss}|\mathcal{N}(0,1)) + KL(\mathbf{Z}_{su}|\mathcal{N}(0,1)) \\ + KL(\mathbf{Z}_{ff}|\mathcal{N}(0,1)) + KL(\mathbf{Z}_{fu}|\mathcal{N}(0,1)) \quad (8)$$

$$L_{rec} = \|\mathbf{A}'_1 - \mathbf{A}_1\|_2 + \|\mathbf{A}'_2 - \mathbf{A}_2\|_2 \quad (9)$$

$$L_{cos} = \frac{\mathbf{Z}_{su} \cdot \mathbf{Z}_{fu}}{\|\mathbf{Z}_{su}\| * \|\mathbf{Z}_{fu}\|} \quad (10)$$

$$L_{cls} = -\mathbf{y} \cdot \log(C(\mathbf{A}_m)) \quad (11)$$

here, \mathbf{y} is the one-hot vector that represents the truth label.

3 Experimental Results

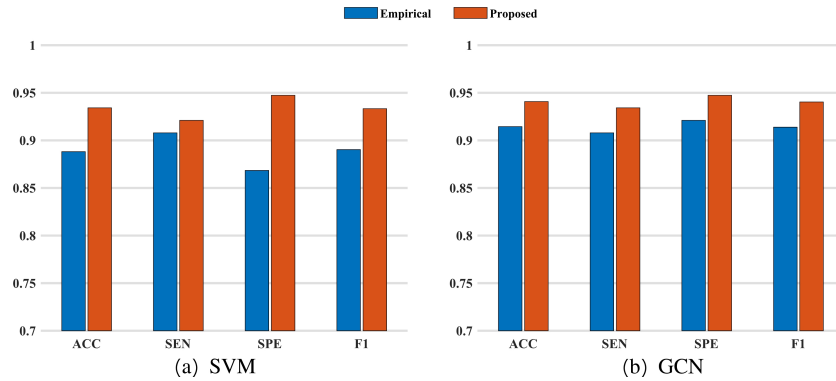
In this study, we selected subjects with both fMRI and DTI from the Alzheimer’s Disease Neuroimaging Initiative (ADNI) dataset. Three stages during the AD progression are considered: normal control (NC), early mild cognitive impairment (EMCI), and late mild cognitive impairment (LMCI). To remove the impact of the imbalanced labels, 76 subjects are selected for each stage. The GRETNA and PANDA toolboxes are utilized to preprocess the fMRI and DTI, respectively. Detailed procedures are described in the work [34]. The final outputs of the pre-processing operation are FC and SC.

The model is trained on the Ubuntu 18.04 platform with the TensorFlow tools. The optimization algorithm is Adam, where the weight decay and momentum rates are 0.01 and (0.9, 0.99). Two binary classification tasks (i.e., NC vs. EMCI and EMCI vs. LMCI) are conducted to evaluate the model’s performance. Three methods are introduced to compare the classification performance of FC and SC. These methods are as follows: (1) DCNN [44], (2) MVGCN [45], (3) JNML [46], and (4) Ours.

Table 1. Comparison of classification performance using different fMRI-DTI fusing methods(%).

Methods	NC vs. EMCI				EMCI vs. LMCI			
	ACC	SEN	SPE	F1	ACC	SEN	SPE	F1
DCNN	83.55	84.21	82.89	83.66	87.50	86.84	88.15	87.41
MVGCN	87.50	88.15	86.84	87.58	90.78	89.47	92.10	90.66
JNML	88.15	89.47	86.84	88.31	92.10	90.78	93.42	92.00
Ours	90.78	92.10	89.47	90.90	93.42	92.10	94.73	93.33

The classification results are presented in Table 1. Our model achieves the best classification performance among the compared methods. The best results for NC vs. EMCI are an ACC value of 90.78%, SEN value of 92.10%, SPE value of 89.47%, and a F1 value of 90.90%; the task of EMCI vs. LMCI yields the best results in terms of ACC (93.42%), SEN (92.10%), SPE (94.73%), and F1 (93.33%). The same phenomenon can be observed by comparing the generated SFC and the empirical SFC. As shown in Fig. 2, the generated SFCs are classified more precisely than the empirical SFCs.

**Fig. 2.** Classification comparison between the generated and empirical SFCs using (a) SVM classifier, and (b) GCN classifier.

To analyze the MCI-related brain regions and connections, we average the generated SFCs for each group (i.e., NC, EMCI, and LMCI) and compute the connectivity difference between adjacent stages. Positive values indicate increased brain connections, and negative values indicate decreased brain connections. We then select important connections by setting a threshold of 75 percent quantile. These connectivity-related ROIs are displayed in Fig. 3. It shows some abnormal ROI distribution patterns when the LMCI stage occurs. In Fig. 4, the top five connections in both decreased and increased situations are presented. The left of each subplot is a qualitative view, and the right of each subplot is a quantitative view with altered connection strength. From NC to EMCI, the top

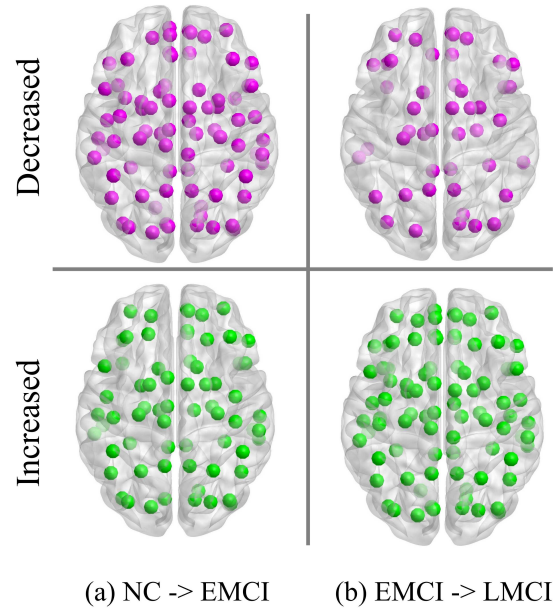


Fig. 3. Spatial distribution of important connectivity-related ROIs at different stages of MCI.

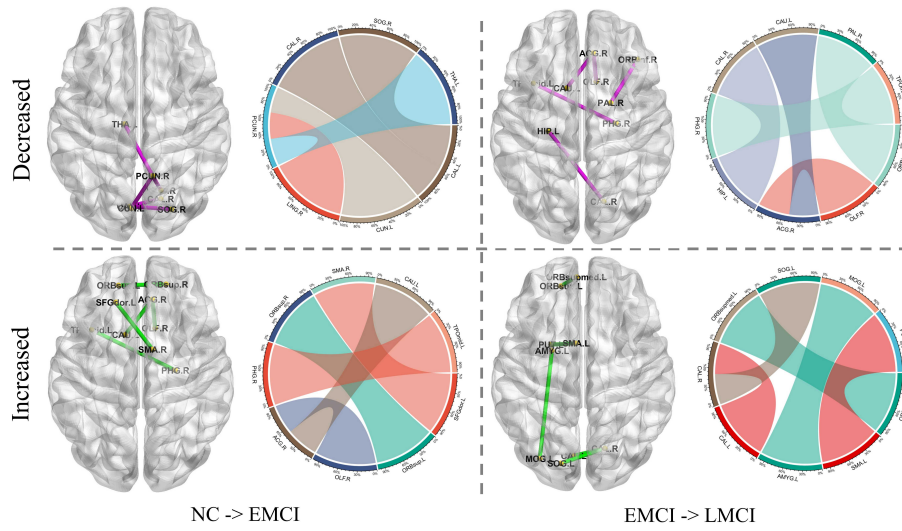


Fig. 4. Qualitative and quantitative visualization of top 5 decreased and increased connections.

five increased connections are: ORBsup.L - ORBsup.R, PHG.R - TPOmid.L, ACG.R - CAU.L, SFGdor.L - SMA.R, and OLF.R - ACG.R; the top five decreased connections are: CAL.L - SOG.R, PCUN.R - THA.L, CAL.L - CAL.R, LING.R - PCUN.R, and CUN.L - PCUN.R. Patients converting from EMCI to LMCI are likely to lose the following five connections: OLF.R - ACG.R, PHG.R - TPOmid.L, ACG.R - CAU.L, HIP.L - CAL.R, and ORBinf.R - PAL.R, while five other connections may be increased: ORBsup.L - ORBsupmed.L, AMYG.L - MOG.L, SMA.L - PUT.L, CAL.R - SOG.L, and CAL.L - CAL.R.

4 Conclusion

This study proposes a model named Hierarchical Structural-functional Connectivity Fusing (HSCF) to build brain structural-functional connectivity matrices and forecast abnormal brain connections by inputting fMRI and DTI. In particular, the graph convolutional networks incorporate prior knowledge into the separators for disentangling each modal information. The additional HRF module can maximize the integration of pertinent and useful data across modalities, which makes the generated structural-functional connectivity more reliable and discriminative in the analysis of cognitive diseases. Study results conducted on the public ADNI database reveal the proposed model’s effectiveness in classification evaluation. The identified abnormal connections will likely be biomarkers for cognitive disease study and treatment.

Acknowledgements This work was supported in part by the Guangdong Social Science Planning Project under Grant GD21YWW01, in part by the Special Fund for Young Teachers in Basic Scientific Research Business Expenses of Central Universities under Grant 2023qntd28, in part by the Young Doctoral Research Start-Up Fund of Hubei University of Economics under Grant XJ22BS28.

References

1. G. Tsentidou, D. Moraitou, and M. Tsolaki, “Cognition in vascular aging and mild cognitive impairment,” *Journal of Alzheimer’s Disease*, vol. 72, no. 1, pp. 55–70, 2019.
2. C. Davatzikos, P. Bhatt, L. M. Shaw, K. N. Batmanghelich, and J. Q. Trojanowski, “Prediction of mci to ad conversion, via mri, csf biomarkers, and pattern classification,” *Neurobiology of aging*, vol. 32, no. 12, pp. 2322–e19, 2011.
3. M. A. Peres, L. M. Macpherson, R. J. Weyant, B. Daly, R. Venturelli, M. R. Mathur, S. Listl, R. K. Celeste, C. C. Guarnizo-Herreño, C. Kearns *et al.*, “Oral diseases: a global public health challenge,” *The Lancet*, vol. 394, no. 10194, pp. 249–260, 2019.
4. H. Keren-Shaul, A. Spinrad, A. Weiner, O. Matcovitch-Natan, R. Dvir-Szternfeld, T. K. Ulland, E. David, K. Baruch, D. Lara-Astaiso, B. Toth *et al.*, “A unique microglia type associated with restricting development of alzheimer’s disease,” *Cell*, vol. 169, no. 7, pp. 1276–1290, 2017.

5. S.-Q. Wang, X. Li, J.-L. Cui, H.-X. Li, K. D. Luk, and Y. Hu, "Prediction of myelopathic level in cervical spondylotic myelopathy using diffusion tensor imaging," *Journal of Magnetic Resonance Imaging*, vol. 41, no. 6, pp. 1682–1688, 2015.
6. Y. Shen, X. Huang, K. S. Kwak, B. Yang, and S. Wang, "Subcarrier-pairing-based resource optimization for ofdm wireless powered relay transmissions with time switching scheme," *IEEE Transactions on Signal Processing*, vol. 65, no. 5, pp. 1130–1145, 2016.
7. E. Gibson, W. Li, C. Sudre, L. Fidon, D. I. Shaker, G. Wang, Z. Eaton-Rosen, R. Gray, T. Doel, Y. Hu *et al.*, "Niftynet: a deep-learning platform for medical imaging," *Computer methods and programs in biomedicine*, vol. 158, pp. 113–122, 2018.
8. S. Wang, Y. Shen, D. Zeng, and Y. Hu, "Bone age assessment using convolutional neural networks," in *2018 International conference on artificial intelligence and big data (ICAIBD)*. IEEE, 2018, pp. 175–178.
9. S. Wang, Y. Shen, C. Shi, P. Yin, Z. Wang, P. W.-H. Cheung, J. P. Y. Cheung, K. D.-K. Luk, and Y. Hu, "Skeletal maturity recognition using a fully automated system with convolutional neural networks," *IEEE Access*, vol. 6, pp. 29 979–29 993, 2018.
10. J. Hong, Z. Feng, S.-H. Wang, A. Peet, Y.-D. Zhang, Y. Sun, and M. Yang, "Brain age prediction of children using routine brain mr images via deep learning," *Frontiers in Neurology*, vol. 11, p. 584682, 2020.
11. S. Wang, X. Wang, Y. Shen, B. He, X. Zhao, P. W.-H. Cheung, J. P. Y. Cheung, K. D.-K. Luk, and Y. Hu, "An ensemble-based densely-connected deep learning system for assessment of skeletal maturity," *IEEE Transactions on Systems, Man, and Cybernetics: Systems*, vol. 52, no. 1, pp. 426–437, 2020.
12. S. Hu, W. Yu, Z. Chen, and S. Wang, "Medical image reconstruction using generative adversarial network for alzheimer disease assessment with class-imbalance problem," in *2020 IEEE 6th international conference on computer and communications (ICCC)*. IEEE, 2020, pp. 1323–1327.
13. W. Yu, B. Lei, M. K. Ng, A. C. Cheung, Y. Shen, and S. Wang, "Tensorizing gan with high-order pooling for alzheimer's disease assessment," *IEEE Transactions on Neural Networks and Learning Systems*, vol. 33, no. 9, pp. 4945–4959, 2021.
14. D. Zeng, S. Wang, Y. Shen, and C. Shi, "A ga-based feature selection and parameter optimization for support tucker machine," *Procedia computer science*, vol. 111, pp. 17–23, 2017.
15. Q. Zuo, C.M. Pun, Y. Zhang, H. Wang, and J. Hong, "Multi-resolution Spatiotemporal Enhanced Transformer Denoising with Functional Diffusive GANs for Constructing Brain Effective Connectivity in MCI analysis," *arXiv preprint arXiv:2305.10754*, 2023.
16. Q. Zuo, B. Lei, Y. Shen, Y. Liu, Z. Feng, and S. Wang, "Multimodal representations learning and adversarial hypergraph fusion for early alzheimer's disease prediction," in *Pattern Recognition and Computer Vision: 4th Chinese Conference, PRCV 2021, Beijing, China, October 29–November 1, 2021, Proceedings, Part III 4*. Springer, 2021, pp. 479–490.
17. S. Wang, Y. Shen, W. Chen, T. Xiao, and J. Hu, "Automatic recognition of mild cognitive impairment from mri images using expedited convolutional neural networks," in *Artificial Neural Networks and Machine Learning–ICANN 2017: 26th International Conference on Artificial Neural Networks, Alghero, Italy, September 11–14, 2017, Proceedings, Part I 26*. Springer, 2017, pp. 373–380.

18. S. Wang, Y. Hu, Y. Shen, and H. Li, "Classification of diffusion tensor metrics for the diagnosis of a myelopathic cord using machine learning," *International journal of neural systems*, vol. 28, no. 02, p. 1750036, 2018.
19. J. Hong, S. C.-H. Yu, and W. Chen, "Unsupervised domain adaptation for cross-modality liver segmentation via joint adversarial learning and self-learning," *Applied Soft Computing*, vol. 121, p. 108729, 2022.
20. B. Lei, E. Liang, M. Yang, P. Yang, F. Zhou, E.-L. Tan, Y. Lei, C.-M. Liu, T. Wang, X. Xiao *et al.*, "Predicting clinical scores for alzheimer's disease based on joint and deep learning," *Expert Systems with Applications*, vol. 187, p. 115966, 2022.
21. D. Hirjak, M. Rashidi, K. M. Kubera, G. Northoff, S. Fritze, M. M. Schmitgen, F. Sambataro, V. D. Calhoun, and R. C. Wolf, "Multimodal magnetic resonance imaging data fusion reveals distinct patterns of abnormal brain structure and function in catatonia," *Schizophrenia bulletin*, vol. 46, no. 1, pp. 202–210, 2020.
22. Q. Zuo, J. Hu, Y. Zhang, J. Pan, C. Jing, X. Chen, X. Meng, and J. Hong, "Brain Functional Network Generation using Distribution-Regularized Adversarial Graph Autoencoder with Transformer for Dementia Diagnosis," 2023.
23. C. J. Honey, O. Sporns, L. Cammoun, X. Gigandet, J.-P. Thiran, R. Meuli, and P. Hagmann, "Predicting human resting-state functional connectivity from structural connectivity," *Proceedings of the National Academy of Sciences*, vol. 106, no. 6, pp. 2035–2040, 2009.
24. Q. Zuo, H. Tian, R. Li, J. Guo, J. Hu, L. Tang, Y. Di, and H. Kong, "Hemisphere-Separated Cross-Connectome Aggregating Learning via VAE-GAN for Brain Structural Connectivity Synthesis," *IEEE Access*, vol. 11, pp. 48493–48505, 2023.
25. S. Wang, H. Wang, Y. Shen, and X. Wang, "Automatic recognition of mild cognitive impairment and alzheimers disease using ensemble based 3d densely connected convolutional networks," in *2018 17th IEEE International conference on machine learning and applications (ICMLA)*. IEEE, 2018, pp. 517–523.
26. S. Hu, J. Yuan, and S. Wang, "Cross-modality synthesis from mri to pet using adversarial u-net with different normalization," in *2019 international conference on medical imaging physics and engineering (ICMIPE)*. IEEE, 2019, pp. 1–5.
27. S. Wang, H. Wang, A. C. Cheung, Y. Shen, and M. Gan, "Ensemble of 3d densely connected convolutional network for diagnosis of mild cognitive impairment and alzheimer's disease," *Deep learning applications*, pp. 53–73, 2020.
28. S. Hu, B. Lei, S. Wang, Y. Wang, Z. Feng, and Y. Shen, "Bidirectional mapping generative adversarial networks for brain mr to pet synthesis," *IEEE Transactions on Medical Imaging*, vol. 41, no. 1, pp. 145–157, 2021.
29. W. Yu, B. Lei, S. Wang, Y. Liu, Z. Feng, Y. Hu, Y. Shen, and M. K. Ng, "Morphological feature visualization of alzheimer's disease via multidirectional perception gan," *IEEE Transactions on Neural Networks and Learning Systems*, 2022.
30. S. You, B. Lei, S. Wang, C. K. Chui, A. C. Cheung, Y. Liu, M. Gan, G. Wu, and Y. Shen, "Fine perceptive gans for brain mr image super-resolution in wavelet domain," *IEEE transactions on neural networks and learning systems*, 2022.
31. B. Lei, S. Yu, X. Zhao, A. F. Frangi, E.-L. Tan, A. Elazab, T. Wang, and S. Wang, "Diagnosis of early alzheimer's disease based on dynamic high order networks," *Brain Imaging and Behavior*, vol. 15, pp. 276–287, 2021.
32. Q. Zuo, B. Lei, N. Zhong, Y. Pan, and S. Wang, "Brain Structure-Function Fusing Representation Learning using Adversarial Decomposed-VAE for Analyzing MCI," *arXiv preprint arXiv:2305.14404*, 2023.

33. Q. Zuo, L. Lu, L. Wang, J. Zuo, and T. Ouyang, "Constructing brain functional network by adversarial temporal-spatial aligned transformer for early ad analysis," *Frontiers in Neuroscience*, vol. 16, 2022.
34. Q. Zuo, B. Lei, S. Wang, Y. Liu, B. Wang, and Y. Shen, "A prior guided adversarial representation learning and hypergraph perceptual network for predicting abnormal connections of alzheimer's disease," *arXiv preprint arXiv:2110.09302*, 2021.
35. Y. Zong, C. Jing, and Q. Zuo, "Multiscale autoencoder with structural-functional attention network for alzheimer's disease prediction," in *Pattern Recognition and Computer Vision: 5th Chinese Conference, PRCV 2022, Shenzhen, China, November 4–7, 2022, Proceedings, Part II*. Springer, 2022, pp. 286–297.
36. J. Hong, Y.-D. Zhang, and W. Chen, "Source-free unsupervised domain adaptation for cross-modality abdominal multi-organ segmentation," *Knowledge-Based Systems*, vol. 250, p. 109155, 2022.
37. S. Yu, S. Wang, X. Xiao, J. Cao, G. Yue, D. Liu, T. Wang, Y. Xu, and B. Lei, "Multi-scale enhanced graph convolutional network for early mild cognitive impairment detection," in *Medical Image Computing and Computer Assisted Intervention–MICCAI 2020: 23rd International Conference, Lima, Peru, October 4–8, 2020, Proceedings, Part VII 23*. Springer, 2020, pp. 228–237.
38. S. Hu, Y. Shen, S. Wang, and B. Lei, "Brain mr to pet synthesis via bidirectional generative adversarial network," in *Medical Image Computing and Computer Assisted Intervention–MICCAI 2020: 23rd International Conference, Lima, Peru, October 4–8, 2020, Proceedings, Part II 23*. Springer, 2020, pp. 698–707.
39. L. Liu, Y.-P. Wang, Y. Wang, P. Zhang, and S. Xiong, "An enhanced multi-modal brain graph network for classifying neuropsychiatric disorders," *Medical Image Analysis*, vol. 81, p. 102550, 2022.
40. L. Zhang, L. Wang, J. Gao, S. L. Risacher, J. Yan, G. Li, T. Liu, D. Zhu, A. D. N. Initiative *et al.*, "Deep fusion of brain structure-function in mild cognitive impairment," *Medical image analysis*, vol. 72, p. 102082, 2021.
41. S.-Q. Wang, "A variational approach to nonlinear two-point boundary value problems," *Computers & Mathematics with Applications*, vol. 58, no. 11-12, pp. 2452–2455, 2009.
42. L.-F. Mo and S.-Q. Wang, "A variational approach to nonlinear two-point boundary value problems," *Nonlinear Analysis: Theory, Methods & Applications*, vol. 71, no. 12, pp. e834–e838, 2009.
43. D. P. Kingma, M. Welling *et al.*, "An introduction to variational autoencoders," *Foundations and Trends® in Machine Learning*, vol. 12, no. 4, pp. 307–392, 2019.
44. J. Atwood and D. Towsley, "Diffusion-convolutional neural networks," *Advances in neural information processing systems*, vol. 29, 2016.
45. X. Zhang, L. He, K. Chen, Y. Luo, J. Zhou, and F. Wang, "Multi-view graph convolutional network and its applications on neuroimage analysis for parkinson's disease," in *AMIA Annual Symposium Proceedings*, vol. 2018. American Medical Informatics Association, 2018, p. 1147.
46. B. Lei, N. Cheng, A. F. Frangi, E.-L. Tan, J. Cao, P. Yang, A. Elazab, J. Du, Y. Xu, and T. Wang, "Self-calibrated brain network estimation and joint non-convex multi-task learning for identification of early alzheimer's disease," *Medical image analysis*, vol. 61, p. 101652, 2020.